The Higher-order Structure of Chromatin: Evidence for a Helical Ribbon Arrangement

C. L. F. WOODCOCK, L.-L. Y. FRADO, and J. B. RATTNER*
Department of Zoology, University of Massachusetts, Amherst, Massachusetts 01003-0027 and
**Department of Anatomy, Faculty of Medicine, University of Calgary, Calgary, Alberta, Canada T2N 4N1*

ABSTRACT Both intact and nuclease-isolated chromatin fibers have been examined at different degrees of salt-induced compaction, using a variety of preparation techniques. The results suggest that the initial folding step in nucleosome packing involves the formation of a zig-zag ribbon as has been proposed by others (Thoma F., T. Koller, and A. Klug, 1979, *J. Cell Biol.*, 83:403–427; Worcel A., S. Strogartz, and D. Riley, 1981, *Proc. Natl. Acad. Sci. USA*, 78:1461–1465), and that subsequent compaction occurs by coiling of the ribbon to form a double helical structure. This type of folding generates a fiber in which the nucleosome–nucleosome contacts established in the zig-zag ribbon are maintained and in which the histone H1 molecules occupy equivalent sites. The diameter of the fiber is not dependent upon the nucleosome repeat length.

Direct mass values for individual isolated fibers obtained from electron scattering measurements showed that the mass per length was dependent on ionic strength, and ranged from 6.0×10^4 daltons/nm at 10 mM NaCl to 27×10^4 daltons/nm at 150 mM salt. These values are equivalent to 2.5 nucleosomes/11 nm at 10 mM NaCl and to 11.6 nucleosomes/11 nm at 150 mM salt and are consistent with the range of packing ratios for the proposed helical ribbon.

Although the first level of DNA packing into nucleosomes is now well established (reviewed in references 12, 14, and 17), the details of the higher order(s) of folding, which predominate in interphase nuclei and chromosomes, are still incompletely understood (12, 17, 28). There is general agreement that the next hierarchical structure above the nucleosome is the "30-nm" chromatin fiber that has been widely observed in thin sections of intact cells and whole mount preparations (12, 14, 28). Studies of the arrangements of nucleosomes in these fibers are facilitated by the reversible salt-induced transition between the relaxed beaded chain of nucleosomes and the 30-nm fiber (9, 35, 36). Electron micrographs of chromatin undergoing this transition often show a fairly regular zig-zag pattern of chromatosome–linker DNA–chromatosome (36, 46), but as compaction proceeds, the individual nucleosomes are no longer resolved and their arrangement in the 30-nm fiber becomes less accessible to direct observation. However, a substantial body of data concerning the biophysical and biochemical properties of both compact and relaxed chromatin has been accumulated, which places many constraints on their possible architecture (reviewed in references 12 and 17).

On the basis of such data, a number of models of the 30-nm chromatin fiber have been proposed. Most of these models have incorporated a superhelical or solenoidal arrangement in which the nucleosomes are arranged helically, and the linker DNA continues in the same helical path established in the nucleosome (10, 18, 19, 36, 45). A second model, based principally on morphological evidence, suggests that clusters or "superbeads" of nucleosomes in some undefined arrangement are strung together to make up the 30-nm fiber (23, 27, 32, 33, 47, 48). A third proposal suggests that the underlying architecture is a flat zig-zag ribbon of nucleosomes which is twisted to generate the 30-nm fiber (34, 46).

In this communication we show that with improved specimen preparation conditions, it is possible to resolve additional details of fiber structure both in spread nuclei and isolated polynucleosomes. The micrographs are consistent with an arrangement based not on a simple solenoid or superhelix, but, as in the proposal of Worcel et al. (46), on a zig-zag ribbon. To form the 30-nm fiber, the ribbon is coiled (as though around a cylinder), forming a structure in which both the linker DNA and the faces of the core particles have a similar orientation with respect to the fiber axis.

THE JOURNAL OF CELL BIOLOGY · VOLUME 99 JULY 1984 42–52

MATERIALS AND METHODS

Preparation of Intact Fibers: Mouse L_{929} cells from the American Type Tissue Collection were grown in Jokliks suspension medium supplemented with 10% fetal calf serum. Chicken cell line MSB (obtained from Harold Weintraub) was grown in RPMI 1620 medium (Gibco Laboratories, Grand Island Biological Co., Grand Island, NY) supplemented with 10% fetal calf serum. Mitotic cells were obtained from cultures treated with colcemid (Gibco Laboratories) at a final concentration of 0.05 μg/ml for 2–3 h and harvested by selective detachment. Interphase cells were obtained from untreated cultures. Cells were lysed in culture medium, pH 7.2, either with 0.1% Nonidet P-40 or by vortexing with glass beads, prepared for electron microscopy as described by Rattner and Hamkalo (24, 25), and examined in a Hitachi HC11-500H electron microscope (Hitachi American, Ltd., NY) operated at 50 kV.

Preparation of Polynucleosomes: Chromatin fibers were isolated by a modification of the method of Ruiz-Carrillo et al. (29). Isolated chicken erythrocyte nuclei (29) were digested for 30 min at 5–6°C with 20–50 U of micrococcal nuclease (Worthington Biochemical Corp., Freehold, NJ) per mg of DNA in buffer A (90 mM KCl, 30 mM NaCl, 0.5 mM spermidine, 0.15 mM spermine, 10 mM triethanolamine-HCl, pH 7.3) supplemented with 1 mM $CaCl_2$. The reaction was stopped on ice by adding 2.5 mM EDTA and 0.1 mM phenylmethylsulfonyl fluoride, pH 8.0, and the nuclei were pelleted and resuspended in buffer C (1 mM EDTA, 10 mM triethanolamine HCl, 0.4 mM phenylmethylsulfonyl fluoride, pH 7.3) containing 140 mM NaCl. Extraction of the chromatin fragments was carried out by the slow addition of buffer C to a final NaCl concentration of 50 mM followed by stirring gently overnight at 4°C. Centrifugation of the suspension yielded a clear supernatant containing 5–10% of the nuclear DNA as chromatin fragments with a median size of ~150 nucleosomes (as determined from direct counts of electron microscope preparations).

Electron Microscopy: Polynucleosomes in buffer C containing 50 mM NaCl were adjusted either directly or through dialysis to the appropriate NaCl or $MgCl_2$ concentration, and then fixed with 1% formaldehyde for at least 12 h at 4°C. For effective adhesion of polynucleosomes to mica, the salt concentration of the fixed samples was raised if necessary (42) before application to freshly cleaved mica fragments. After 3 min for adhesion, the mica surfaces were washed with water, then 2% uranyl acetate, and again extensively with water before being allowed to air-dry. In some cases, the uranyl acetate step was omitted and/or treatment with 5–20% glycerol preceded the drying step. After drying, the mica fragments were shadowed lightly with platinum-carbon (from pellets) at an angle of 17°, using both unidirectional and rotary modes, and finally coated with carbon.

Replicas were floated on a dilute hydrofluoric acid solution, and transferred to 400-mesh grids. Some replicas were additionally treated with 70% H_2SO_4 and commercial bleach to remove adhering chromatin, but this step did not markedly affect the final image. Grids were examined with a Siemens 102 microscope (Siemens Corp., Iselin, NJ), using the tilted-beam, dark-field mode at 60 kV. Parallel samples placed on glow-discharged carbon films were prepared similarly, except that the carbon replication step was omitted.

Freeze Drying: Samples prepared on mica or carbon coated grids were blotted, then plunged rapidly into a liquid nitrogen slurry prepared by drawing a vacuum on a Dewar of liquid nitrogen. The frozen samples were transferred rapidly to a metal boat containing liquid nitrogen which was inserted into a ion-pumped vacuum chamber (Varian Associates, Palo Alto, CA). Freeze drying was allowed to proceed overnight at −60 to −80°C and 10^{-7} Torr, the sample temperature being maintained via a liquid nitrogen feedthrough. Shadowing and replication were then carried out as described above, except that some samples were kept at −80°C during the shadowing operation.

Negative Staining: Fixed or unfixed samples were applied to glow-discharged carbon-coated grids, rinsed with several drops of 2% aqueous uranyl acetate, blotted, and air-dried.

Scanning Transmission Electron Microscopy (STEM):[1] Chromatin samples for mass analysis were adjusted to the desired salt concentration, fixed for 24 h with 0.1% glutaraldehyde or 1.0% formaldehyde, and transported to the Brookhaven Laboratory on ice. They were then placed on glow-discharged carbon films and washed, tobacco mosaic virus was added, and the grids were freeze-dried and examined unstained as described (43). Large-angle scattering was recorded on magnetic tape during the first scan using a dose of 10–25$e^-/Å^2$, and a pixel size of 20.3 or 10.1Å. Mass values were computed by summing the scattering values over a length of chromatin fiber, subtracting background (scattering from the carbon substrate), and converting to daltons using the tobacco mosaic virus internal standard (43).

[1] *Abbreviation used in this paper:* STEM, scanning transmission electron microscopy.

RESULTS

Fibers from Interphase Nuclei and Chromosome

Intact chromatin fibers can be released from interphase or metaphase cells by either gentle lysis in a solution of 0.1% Nonidet P-40 in tissue culture media or mechanical disruption (24, 25). Samples obtained from various cell types prepared in this manner and processed for electron microscopy as described (24) reveal a consistent arrangement of nucleosomes along extended stretches of the intact fiber. Particularly prominent are regions of parallel rows of nucleosomes that extend along the fiber axis (Fig. 1 *a–e*) as previously reported (24). These rows appear to be formed by the compact folding of a zig-zag array of nucleosomes, which is apparent in more dispersed regions of the fibers (Fig. 1 *a*), as has been observed by others (46). The rows may be condensed so that only a pair of electron opaque lines (the nucleosomes) with an electron-lucent line (the linkers) are apparent (Fig. 1 *c–g*). However, a small degree of relaxation reveals that the nucleosomes within the compact parallel rows are oriented so that the "tops" and "bottoms" of adjacent nucleosome cylinders are in contact with each other (Fig. 1 *a, h, i*). Further relaxation invariably results in the nucleosome faces adhering to the carbon film as is usual in electron microscope preparations (42; Fig. 1 *a–f*). However, the parallel-row configuration can be maintained even with this change in nucleosome orientation (Fig. 1 *b, d, e*). A common feature of fibers that show extensive parallel row pattern is an occasional sharp discontinuity in the compact zig-zag, which seems to arise from the loss of one nucleosome–nucleosome contact point (Fig. 1 *d, e*, arrows). Loss of the parallel-row orientation within these segments results in the appearance of "superbeads" (Fig. 1 *d, e*), which become more prominent as such fiber preparations undergo relaxation (25). In some regions, the complete ribbon appears to undergo coiling (both left- and right-handed) about the fiber axis (Fig. 1 *c, g*). This arrangement is even more pronounced in negatively stained preparations of mechanically lysed samples (Fig. 1 *h, i*), indicating that the face-to-face orientation of the nucleosomes is maintained within the coiled ribbon.

Isolated Polynucleosomes

Polynucleosomes isolated from chicken erythrocyte nuclei under "physiological" salt conditions using the method of Ruiz-Carrillo et al. (29) were observed in different stages of relaxation by lowering the monovalent cation concentration. These preparations contained the full complement of core and linker histones both before and after formaldehyde fixation (data not shown). In some experiments the effects of magnesium ions were determined by dialysis to the appropriate $MgCl_2$ concentration in the absence of other ions. The use of freshly cleaved mica substrates, followed by light platinum-carbon shadowing, replication, and dark-field electron microscopy, was found to produce substantial gains in specimen detail as compared with direct staining or shadowing on carbon substrates. However, mild aldehyde fixation was necessary to prevent disruptive surface effects (20, 36, 42). Freeze drying of specimens after quenching in liquid nitrogen slurry produced comparable results but less consistently than air drying, except in the case of fully relaxed chromatin, where freeze drying clearly helped to avoid structural collapse.

LOW IONIC STRENGTH: At ionic strengths of 10 mM NaCl or below and 10 μM $MgCl_2$ or below, the chromatin

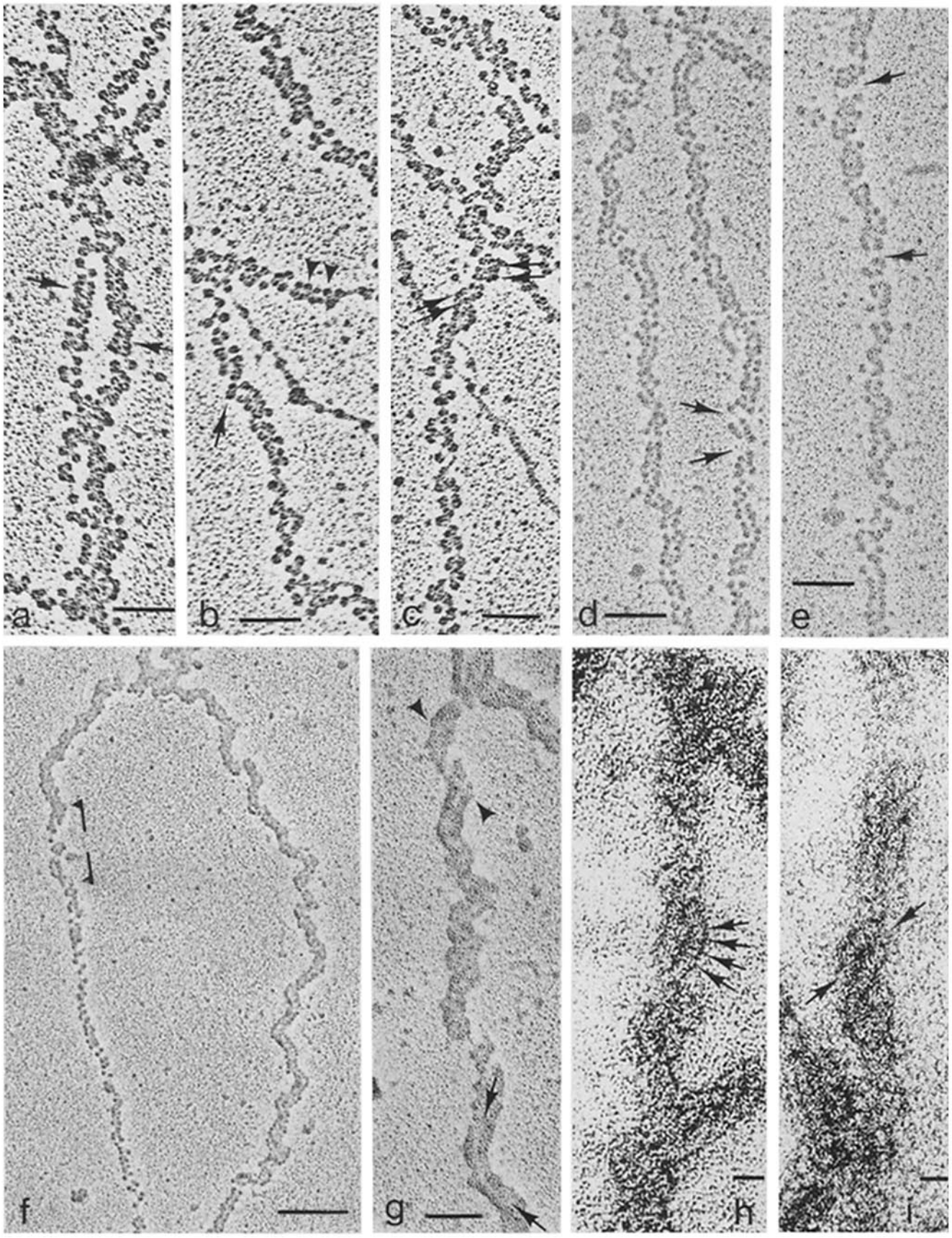
a
b
c
d
e
f
g
h
i

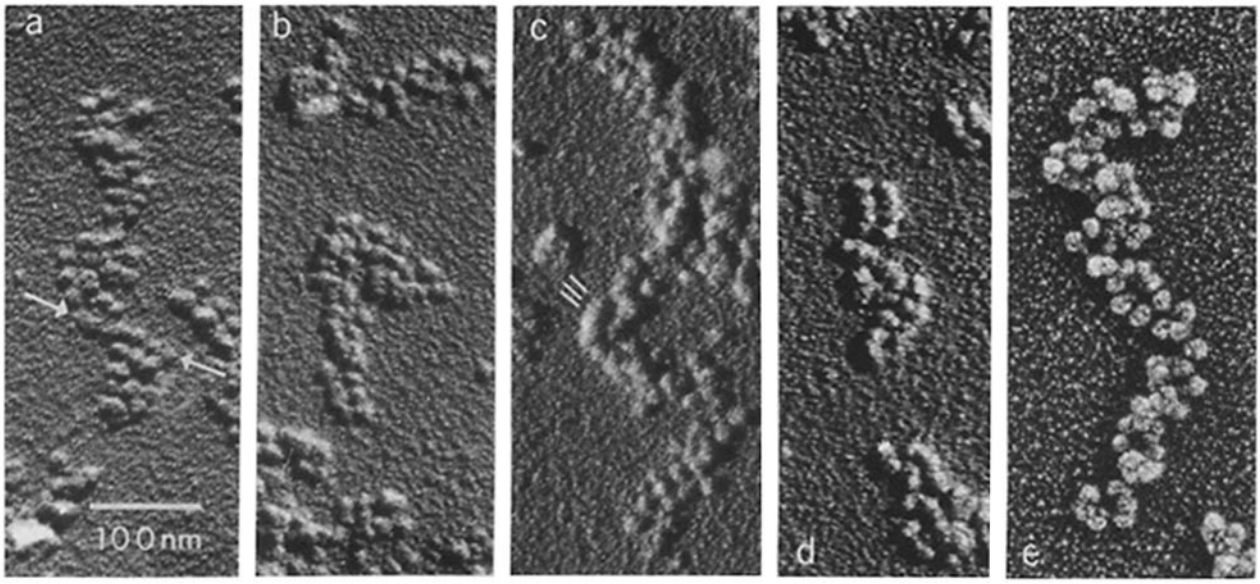

FIGURE 2 Chicken erythrocyte chromatin fibers fixed in 10 mM NaCl, air-dried and replicated on mica after uranyl acetate staining, and viewed with dark-field optics. e is rotary shadowed whereas the others are unidirectionally shadowed. (*a*) Loosely compacted fiber with most nucleosomes adhering *en face* to the substrate. An array of nucleosomes with face-to-face stacking is indicated by the arrows. (*b*) The two-nucleosome-wide ribbon is illustrated. Most of the nucleosomes are adhering face-to-face with each other. (*c*) White lines indicate a clear case of face-to-face contact between nucleosomes in the ribbon. (*d*) The center fiber appears to be undergoing a loose left-handed coiling; the ribbon pattern is clear in the upper portion. (*e*) Loose coiling is apparent in this rotary-shadowed fiber. × 150,000.

fibers were relaxed, revealing individual nucleosomes (Figs. 2*a* and 3). (The Mg^{++} value should be regarded as approximate in that it refers to the $MgCl_2$ concentration outside the dialysis bag.) Many of the fibers appeared in the form of two parallel rows of nucleosomes, but without the regularity seen in intact fibers (Fig. 1). Again, two types of nucleosome orientation were seen: those with one face attached to the substrate, and those with the edge attached to the substrate. In the latter cases (Fig. 2*a*, arrows, Fig. 2*c*, lines), the nucleosomes were always attached face to face with each other. Loose coiling of the whole fiber was often apparent—this is particularly clear in Fig. 2*d*, and in the rotary shadowed Fig. 2*e*.

MEDIUM IONIC STRENGTH: At ~20 mM NaCl or 50 μM $MgCl_2$, chromatin fibers showed partial compaction, and in most cases, loss of resolution of individual nucleosomes (Fig. 3). However, it was at this intermediate salt concentration that indications of the mode of nucleosome packing were most evident, with distinct helical patterns (both left- and right-handed) being observed in numerous instances. The diameter of the chromatin fibers in 20 mM NaCl had a range of 15–50 nm with a mean of 31 nm indicating that the structures being examined were comparable in size to the first level of nucleosome packing observed by others. (These values have been corrected for the increase in size produced by the replication process: individual nucleosomes had a mean diameter of 19 nm under our preparation conditions, indicating that linear measurements should be reduced by 8 nm.) In a few cases, it was also possible to see details within the gyres of a helix. These took the form of cross-striations approximately perpendicular to the gyre, and 6–8 nm apart (Fig. 3*b*). Such observations suggest that the gyres are composed of nucleosomes with the cylinder ends touching as in the compact zig-zag (Figs. 1*a*, *h* and 2*c*), again implying that the nucleosome–nucleosome contacts of the compact zig-zag remain intact in the 30-nm chromatin fiber.

To determine which structures would be consistent with the observed helices, measurements of fiber diameter, helix

FIGURE 1 (*a–c*) Chromatin fibers released from MSB metaphase cells by detergent lysis. *a* illustrates the folding of the zig-zag nucleosome array into a two-parallel-row orientation. Regions showing face-to-face stacking of nucleosomes within one or both of the rows are indicated by single arrows. *b* illustrates that the two-parallel-row arrangement is maintained in relaxed regions where the face-to-face interaction is lost (double arrowheads). A simple twist of the ribbon is indicated by the single arrow. *c* illustrates several coils of the ribbon (double arrows). Bars, 50 nm. × 220,000. (*d* and *e*) Interphase chromatin fibers released from a mouse L_{929} cell by detergent lysis illustrating that the parallel-row arrangement is a general feature that extends for long distances. Occasional discontinuities are indicated by the arrows. Within these discontinuities the parallel-row orientation may be lost giving rise to a superbead appearance (*e*, arrows). Bars, 100 nm. × 220,000. (*f*) Metaphase chromatin fiber released from a mouse L_{929} cell by mechanical lysis. The fiber illustrates the transition from a loosely packed ribbon to a compact fiber (region in brackets). Bar, 100 nm. × 130,000. (*g*) Interphase chromatin fiber released from a mouse L_{929} cell by mechanical lysis. A twist of the fiber is indicated by the arrowheads and the arrows indicate the electron translucent (linker) region between adjacent rows of tightly packed nucleosomes. Bar, 50 nm. × 100,000. (*h* and *i*) Negatively stained chromatin fibers from mouse L_{929} metaphase chromosomes obtained by mechanical lysis in which a coiling of the parallel rows is evident. The face-to-face contacts (arrows in *h*) established within the ribbon appear to be maintained as the ribbon coils about the fiber axis. Arrows in *i* indicate a prominent gyre. Bars, 10 nm. × 500,000.

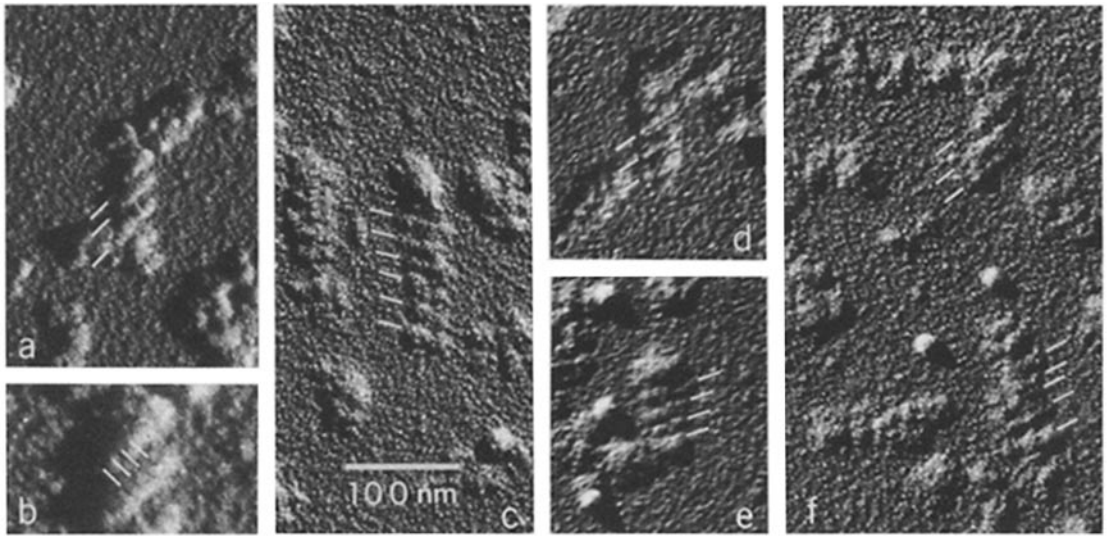

FIGURE 3 Chicken erythrocyte chromatin fibers fixed in 20 mM NaCl, prepared as in Fig. 2. (*a*) Coiled ribbon arrangement is clearly seen. (*b*) Higher magnification of *a* showing cross-striations which are interpreted as delineating adjacent face-to-face nucleosomes. (*c–f*) Examples of helical fibers that were not pretreated with uranyl acetate, and so appear more flattened. Helical patterns are still evident (lines). (*a* and *c–f*) × 150,000; (*b*) × 300,000.

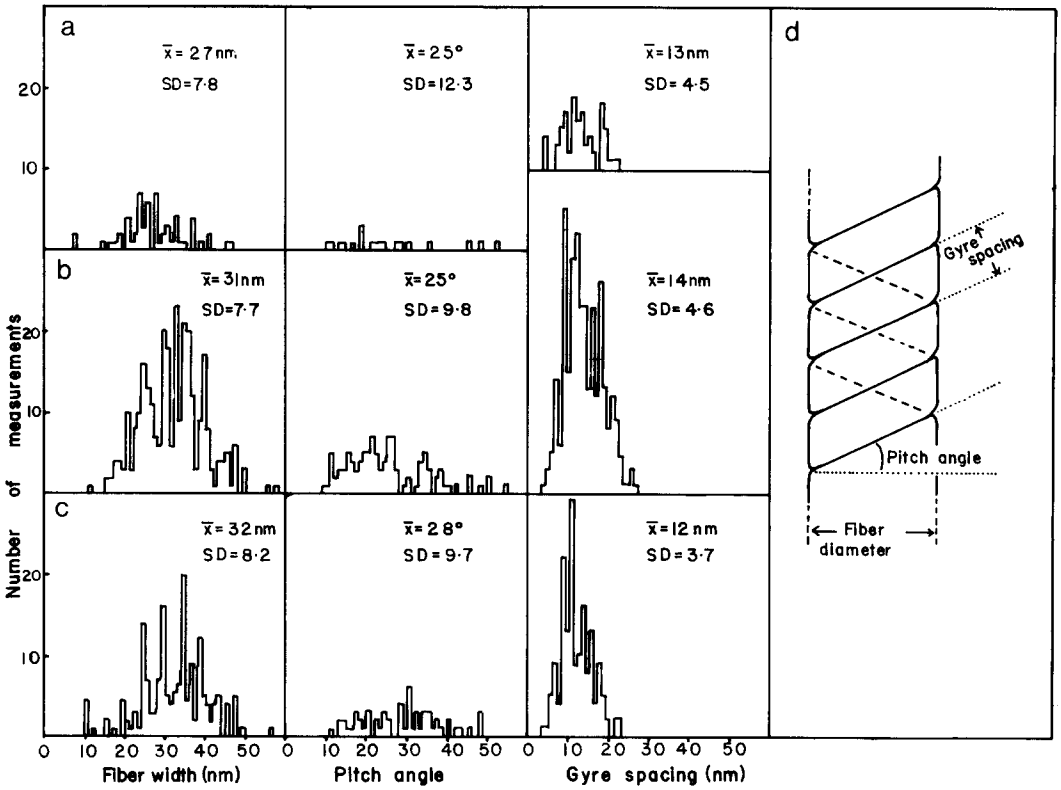

FIGURE 4 (*a–c*) Histograms of helix parameters from fibers such as those shown in Figs. 2 and 3. (*a*) Chromatin fixed in 10 mM NaCl, prestained with uranyl acetate. (*b*) Chromatin fixed in 20 mM NaCl, prestained with uranyl acetate. (*c*) Chromatin fixed in 20 mM NaCl, no prestaining. (*d*) Average helix measurements presented graphically. The figure also defines the three parameters, fiber diameter, pitch angle, and gyre spacing used in *a–c* and the text.

pitch, and helix gyre spacing were tabulated (Fig. 4 *a–d*). Helix pitch was estimated using the angle between the gyres and a perpendicular to the fiber axis (see Fig. 4 *d*) and were confined to fibers in which this parameter could be measured unequivocally; this accounts for the smaller number of angle data points (Fig. 4 *a–c*). At 20 mM NaCl (Fig. 4 *b*) the mean pitch angle was ~25°, with a standard deviation of ~10°, whereas the gyre spacing was more consistent, with a mean value of 14 nm (because a shadow technique was used, this measurement does not necessarily represent gyre width). Similar values were obtained for helical structures observed in 10 mM NaCl (Fig. 4 *a*).

Fig. 4 *d* has been drawn to illustrate a helix with the average diameter, gyre spacing, and pitch. It is clear from the relationship between pitch and fiber diameter that a simple helix is an unlikely arrangement, but that a double-helical array, or two-start helix is consistent with the data.

HIGHER SALT CONCENTRATIONS: Between 50 and 100 mM NaCl, or $MgCl_2$ concentrations above 100 μM, further compaction of the chromatin fibers was noted, but the helical pattern was still observed, though less frequently (Fig. 5). The helix parameters were little changed, although there was a distinct increase in fiber diameter which now showed a mean value of 40 nm and a reduction in mean

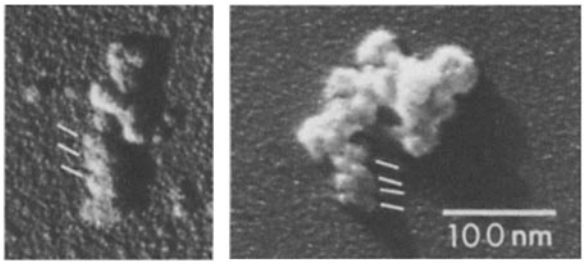

FIGURE 5 Chicken erythrocyte chromatin fibers fixed in 100 mM NaCl and prepared as in Fig. 2. Helical structures are again seen (white lines). × 150,000.

pitch angle to 22° (not shown).

DIVALENT VS. MONOVALENT CATIONS: Although Na^+ and Mg^{++} produced similar degrees of chromatin compaction at the differential concentrations noted, there were quantitative and qualitative differences in the morphology of chromatin fibers with the two ion types. Most obvious was the greater heterogeneity of fiber diameter in Mg^{++}, especially the presence of a class of thinner fibers and thinner areas within fibers that had a 10–20-nm-diam range. The qualitative differences were noticeable increases in morphological heterogeneity, with a greater proportion of irregularly shaped particles.

Some experiments were also carried out on chromatin that had not been exposed to polyamines: again, helical structures were seen with parameters similar to those in Fig. 4 *a–c* (data not shown).

EFFECT OF PREPARATION CONDITIONS ON HELIX PARAMETERS: Fibers showing a helical structure were common only in preparations that had been air- or freeze-dried on mica, or freeze-dried on carbon. These methods usually also included staining with aqueous uranyl acetate after deposition of the chromatin on the substrate, followed by an extensive water rinse. To determine whether the uranyl stain was influencing the final structure, this step was omitted in some experiments. Although the omission of stain altered the appearance of the chromatin (Fig. 3 *c–f*), it did not reduce the frequency of helical forms or significantly alter the pitch angle (Fig. 4 *c*). The main effect of omitting stain was a much greater flattening of the fibers; measurements of shadow length showed that, whereas stained fibers were slightly flattened, with a mean width/height ratio of 1:0.75, unstained material was severely distorted with a width/height ratio of 1:0.1.

The inclusion of glycerol in the final water wash was also explored, since drying from glycerol has been shown to have a protective effect when used in conjunction with a mica substrate (39). For chromatin fibers, glycerol produced no marked changes in diameter, helix parameters, or on the width/height ratio (not shown), but there was a subtle increase in the definition of surface features.

Negative staining with uranyl acetate has been widely used for examining isolated chromatin fibers (e.g., 6, 10, 15, 28), and although it often resolves individual nucleosomes in partially relaxed fibers, there is usually no discernible ordered arrangement. Our observations in using this technique have been similar (44), but occasionally regular helical structures were seen (Fig. 6). In this particular fiber the gyre spacing was 12 nm, and the pitch angle 55° (see Fig. 4 *d* for pitch angle definition).

Mass of Isolated Polynucleosomes

Isolated polynucleosomes, prepared as described, were adjusted to 10, 20, 50, 100, or 150 mM NaCl or KCl, fixed with formaldehyde as described above or with glutaraldehyde (36), and freeze-dried on thin carbon substrates to which tobacco mosaic virus had been added as a mass standard. Large angle electron scattering was then recorded with the Brookhaven STEM (41). It was previously shown for chromatin particles that mass values calculated by this method were very close to those expected (43). The unstained chromatin fibers showed the irregular morphology typical of isolated polynucleosomes (Fig. 7), but there were fairly straight and uniform regions especially at 50 mM NaCl and above, and it was from these that mass measurements were taken. Total scattering from a region was corrected for background (scattering from the carbon substrate), converted to mass using a tobacco mosaic virus-derived calibration factor (43), and expressed as daltons/nanometer. The mass per unit length of the fibers was strongly dependent on salt concentration, ranging from 6.0×10^4 daltons/nm at 10 mM NaCl to 27×10^4 daltons/nm at 150 mM (Table I). At 10 and 20 mM NaCl, the mass values showed the highest variation, with standard deviations approaching 20% of the mean (Table I), but at the higher concentrations, the standard deviations were 10% of the mean or less. This variation reflects the irregularities in the fibers (Fig. 7), rather than inaccuracies in the STEM technique; as the fibers became more regular in morphology with increasing salt, so the mass per unit length was more consistent (Table I). Although the electron beam causes some loss of mass, the low doses used in these experiments results in a loss of 5% or less (43).

The mass per unit length of chromatin fibers is often expressed in terms of the number of nucleosomes per 11 nm,

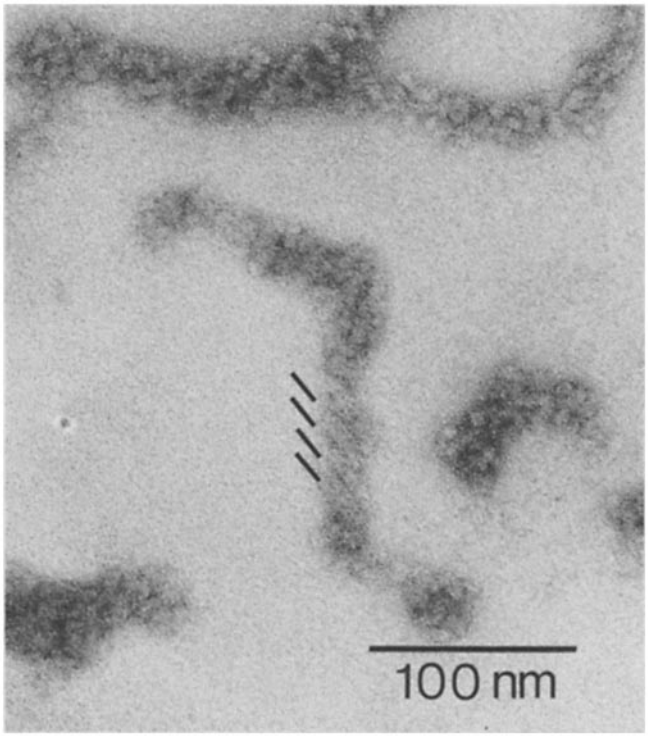

FIGURE 6 Example of the occasional helixlike structure (black lines) seen in unfixed fibers, negatively stained with uranyl acetate. × 270,000.

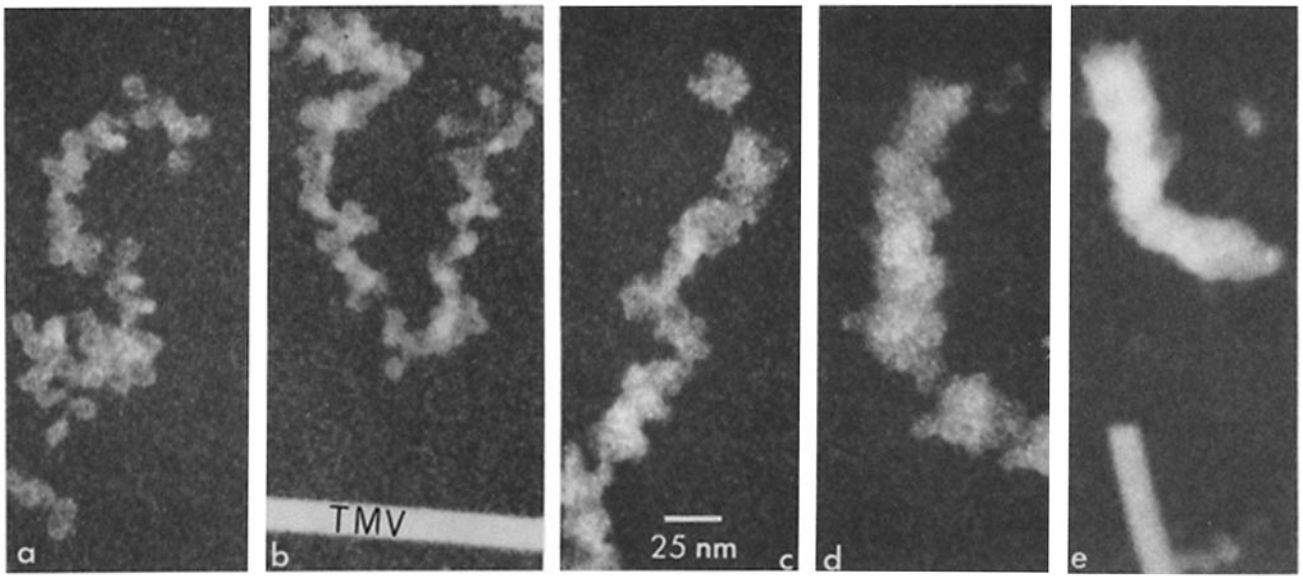

FIGURE 7 Examples of unstained chicken erythrocyte chromatin fibers observed by STEM fixed in (*a*) 10 mM NaCl, (*b*) 20 mM NaCl, (*c*) 50 mM NaCl, (*d*) 100 mM NaCl, (*e*) 150 mM KCl. *TMV*, tobacco mosaic virus standard. × 300,000.

TABLE I

Mass per Unit Length Values for Chromatin Fibers Fixed at Various Salt Concentrations

Monovalent salt concentration	Mass per length (mean ± SD)	Number of nucleosomes per 11-nm length of fiber
mM	*daltons/nm × 10⁴*	
10	6.0 ± 1.3	2.5
20	7.1 ± 1.4	3.1
50	12 ± 1.2	5.2
100	19 ± 1.8	8.2
150	27 ± 0.4	11.6

corresponding to a complete turn of superhelix with an 11-nm pitch. Taking the mass of the chicken erythrocyte nucleosome to be 2.55×10^5 daltons (210 base-pairs [bp] of DNA plus 8 core histones plus one very lysine-rich histone), the number of nucleosomes per 11 nm of chromatin fiber ranges from 2.5 at 10 mM NaCl to 11.6 at 150 mM (Table I).

DISCUSSION

We have shown that under a variety of conditions, isolated and intact chromatin fibers have a distinct helical architecture based on the folding of a nucleosomal ribbon. In all cases, the chromatin was prevented from complete unfolding by maintaining an appropriate salt concentration throughout the preparation. Thus, the structures we observe are not caused by the refolding of relaxed chains of nucleosomes: in the case of structures based on refolded fibers, there is no guarantee that the native conformation will be regenerated, particularly if higher-order folding first requires the establishment of a uniform nucleosomal ribbon. Preparation for electron microscopy may result in morphological changes such as shrinkage (15), and chromatin is particularly susceptible to surface effects (20, 36, 42). To avoid air-drying artifacts, some samples were freeze-dried, and all were stabilized against surface denaturation by mild aldehyde fixation (20, 36, 42). It was reassuring to find that unstained freeze-dried fibers observed with the STEM (Fig. 7) had a mean diameter of 28 nm in 50 mM monovalent ions, very similar to that in replicas of similar air-dried specimens.

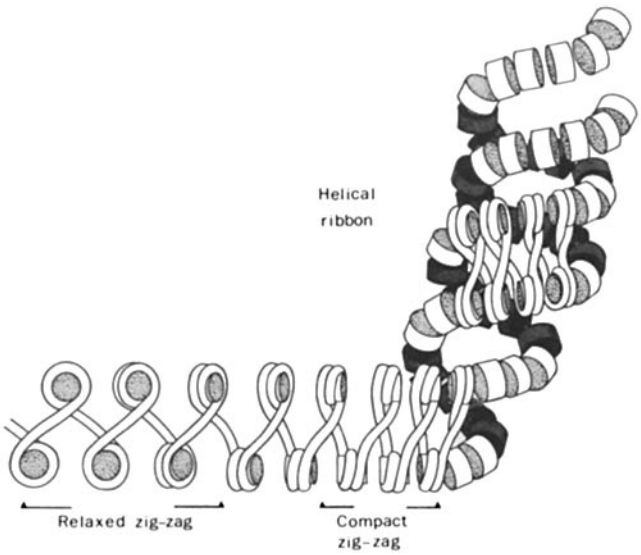

FIGURE 8 Representation of the stages in folding of a nucleosomal chain (*left*) via the zig-zag ribbon into the helical ribbon (*right*) conformation. To avoid confusion, the DNA is shown only in places, and some underlying nucleosomes have been shaded.

An important feature of the micrographs of intact fibers released from nuclei and chromosomes is that there is a smooth transition from the compact zig-zag ribbon to the 30-nm fiber (Fig. 1*f*). This suggests that no major changes in basic structure, especially the loss or addition of nucleosome–nucleosome contacts takes place during the ribbon ⇌ fiber transition. Thus, in the 30-nm fiber, as in the compact ribbon, it seems likely that face-to-face contact between nucleosomes is maintained. In other words, the 30-nm fiber is constructed by folding the zig-zag ribbon in a way that minimizes changes in nucleosome–nucleosome contacts. One method of achieving this, which fits our morphological observations, is shown in Fig. 8.

The Double Helical Ribbon

Simple coiling of the compact zig-zag ribbon creates a double helix with a range of diameters and pitch angles that are dependent on the degree of coiling but independent of the size of the nucleosome repeat. (The nucleosome repeat will affect the width of the ribbon, but not the width of the coil.) As discussed in more detail below, the helical structure shown in Fig. 8 accommodates the full range of nucleosome-packing densities required by our electron scattering measurements.

An alternative way of forming a fiber from the ribbon is to twist the ribbon about its axis. This, however, results in a structure in which the linker DNA strands run more or less perpendicular to the fiber axis, a condition that is difficult to reconcile with recent electric dichroism data (18, 19). Twisting also distorts the ribbon more severely, tending to disrupt the face-to-face contacts between adjacent nucleosomes.

Path of the DNA

Although the precise path of the DNA in the compact ribbon cannot be determined from our morphological data, possible alternatives merit discussion because each imposes different constraints on the construction of the fiber. The simplest case is that in which the DNA makes two complete left-handed turns around a histone core, and then passes across the ribbon (as linker DNA) to a second core (Fig. 9). Clearly, such an arrangement requires a certain minimal length of linker DNA. Space-filling models indicate that the minimum linker length allowable for ribbon formation is ~10 bp (3.4 nm), resulting in a nucleosome repeat of ~176 bp. This repeat size is found in Chinese hamster ovary chromatin (14), although most higher eucaryotes have repeats larger than this (14). One striking exception is the mammalian cerebral cortex neuron with a repeat of ~165 bp (22, 38). Here, the DNA must pass from chromatosome (30) to chromatosome with no linker, and if the DNA is attached to the histone core throughout two complete turns, then any sort of ribbon arrangement would be forbidden. Alternatively, the 166 bp of the chromatosome could consist of 145 bp attached to the histone core, with the remaining 21 bp of DNA unattached, yet partially protected from nuclease attack by H1 (Fig. 10). This would provide an additional ~7-nm of relatively free DNA, allowing ribbon formation even with such short repeats. In this respect, it is worth noting that recent micrographs of cortical neuron chromatin (38) fixed in 5 mM NaCl, an ionic strength at which the chromatosome is stable (36), clearly show stretches of "linker" between nucleosomes. It also appears that these neural cells contain a reduced amount of histone H1. Similarly, H1 seems to be absent from yeast chromatin which also has a small repeat, and larger than expected linkers in electron microscope preparations (26). Perhaps, in these chromatins, the reduction of H1 reflects an accommodation necessary to allow for the higher-order fiber formation observed in these tissues (26).

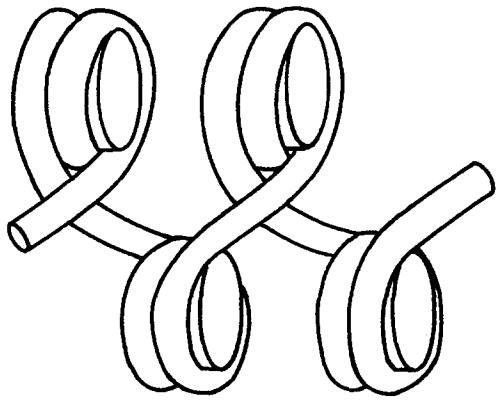

FIGURE 9 DNA path in a simple zig-zag ribbon with $\Delta L = -2$/nucleosome.

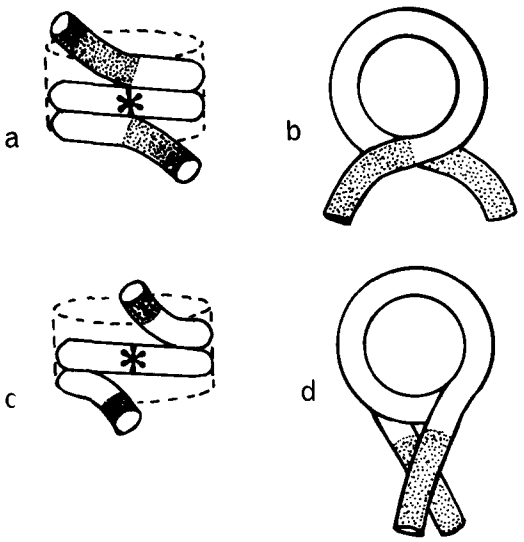

FIGURE 10 Diagram of chromatosomes with two complete turns (166 bp) of DNA attached to the histone core (*a* and *b*) and 1.75 turns (145 bp) of DNA attached to the core (*c* and *d*), showing the additional linker flexibility in the latter arrangement. Stippled areas show true linker; asterisks indicate the putative position of histone H1.

Worcel et al. (46) have proposed a DNA path for the zig-zag ribbon, which results in a linking number change (ΔL) of -1 per nucleosome, as compared with -2 for the arrangement discussed above (Fig. 9). Although the linking number of native SV40 minichromosomes and nucleosomes reconstituted onto circular DNA is -1 per nucleosome (reviewed in references 17 and 40), this could be due to partial unwinding of nucleosomal DNA (40) or a lack of contributions from H1 (31). We feel that the linker path required to generate a linking number of -1 per nucleosome (46) is less attractive since models built with this linker organization do not readily conform to the "relaxed zig-zag" state (Fig. 8).

Location of Histone H1 (H5)

There is considerable evidence that the very lysine-rich histones are located on the chromatosome at the entry/exit point of the DNA (1, 3, 11, 17, 30, 36). If this location is correct, then each H1 molecule would occupy an equivalent position in the helical ribbon, regardless of the overall nucleosome repeat length, or of local variation in DNA linker length. This is clearly in contrast to superhelical structures in which linker length variations result in differing H1 positions within the fiber (18, 19). In the helical ribbon, H1 molecules are neither completely exposed on the outside of the fiber, nor completely hidden in the interior (Figs. 8–10).

Compatibility with Other Measurements

Several groups have reported values for the mass per unit length of chromatin fibers in solution by using light scattering

(7), neutron diffraction (8), hydrodynamic studies (16), and relaxation time after electric field orientation (18). These investigations have yielded values of, or have been compatible with a 30-nm fiber with about six nucleosomes per 11 nm length, suggesting a superhelical or solenoidal arrangement with about six nucleosomes per turn. Our direct mass measurements by electron scattering (Table I) indicate a continuum of nucleosome packing, dependent on salt concentration. Table II shows the mass per length predicted for various ideal cases of nucleosome packing, again using the value of 2.55×10^5 daltons for the mass of the chick erythrocyte nucleosome. At 100 mM monovalent ions and above, the observed mass is considerably higher than that predicted for a six nucleosome per turn solenoid.

The discrepancy between solution studies and our electron scattering data is most probably related to the sampling method. Electron scattering was measured only from selected regions of more or less uniform fiber, whereas solution studies are necessarily averages of the total population. Thus, it seems quite likely that regions of more extended chromatin in the population such as were observed in all our preparations (Fig. 7) could result in lowered mass per unit length values for fibers in solution.

The helical ribbon conformation is able to accommodate the continuous changes in mass per length that were observed with increasing ionic strength, while maintaining nucleosome–nucleosome contacts. At 10–20 mM NaCl, the mass per length (Table I) is intermediate between that expected for the relaxed zig-zag and the compact zig-zag (Fig. 8, Table II), while at 50 mM NaCl, the mass per length is close to that expected for a six nucleosome/turn superhelix (Table II). For the superhelix, further compaction is not possible unless the basic structure is altered; however, the chromatin fiber clearly undergoes further condensation in 100 and 150 mM monovalent ions (Table I), which can be achieved by differing degrees of coiling of the zig-zag ribbon. Examination of space-filling models shows that the helical ribbon can vary continuously in mass per length from 9.2 daltons/nm (uncoiled, compact ribbon) to ~28 daltons/nm (coiled with 25° pitch angle, and ribbon width 25 nm). A similar conclusion can be drawn from theoretical considerations (see Appendix).

TABLE II

Predicted Mass per Unit Length Values for Chromatin Fibers with Various Nucleosome Packing Arrangements

Packing mode	Mass per length
	daltons/nm × 10^4
10-nm fiber—edge-to-edge contact	2.3
	
10-nm fiber—face-to-face contact	4.6
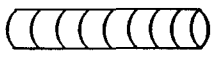	
Zig-zag ribbon, relaxed form	4.6
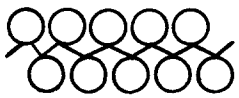	
Zig-zag ribbon, compact form with face-to-face contacts	9.2
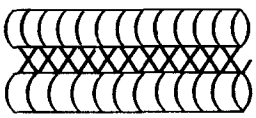	
Solenoid/superhelix, six nucleosomes per turn	13.8
Helical ribbon (Fig. 8)	9.2 (not coiled) to ~28 at pitch angle of 25°

Although fibers in solution can undergo extensive salt-induced compaction, it is not possible to predict the in vivo compaction site since the effective ionic conditions in the nucleus are unknown. Although thin sections of nuclei exposed to 20 mM KCl during fixation showed close-packed nucleosomelike structures in the chromatin fibers (21), estimates of packing density or arrangement have not yet become possible.

From the helical ribbon model, it can be predicted that the nucleosomal and linker DNAs share approximately the same orientation with respect to the fiber axis (in contrast to a twisted ribbon in which the linkers remain more or less perpendicular to the fiber axis). Electric dichroism measurements provide information on DNA orientation within the fiber (16, 17, 19) and so impose constraints upon the relative orientations of nucleosome and linker. Calculations by McGhee at al. (17, 19) based on electric dichroism have indicated the permissible orientations of nucleosome and linker in the 30-nm fiber. For chicken erythrocyte chromatin, the condition under which the nucleosome tilt angle and spacer tilt angle are equal (as predicted by the helical ribbon model) is that both are oriented at ~30° with respect to the fiber axis (17; Fig. 5). As seen from Fig. 4, the mean pitch angle for the helical structures we observe is ~25°, indicating that the proposed model is consistent with electric dichroism data.

Electric dichroism measurements on the 30-nm fiber are usually carried out by using polynucleosomes condensed with magnesium, since the higher ionic strengths of monovalent cation solutions giving similar degrees of compaction are not compatible with the electric fields needed. To determine whether there were any morphological differences between chromatin condensed to equal extent by monovalent or divalent cations, samples were prepared under both conditions. In general, isolated polynucleosomes showed similar morphological features whether condensed by Mg^{++} or Na^+, although when magnesium ions were used to maintain the compact morphology, there was considerably less uniformity in the diameter of the fibers.

One set of data, which seems at variance with the helical ribbon model, is that concerned with the properties of oligonucleosomes. Butler and Thomas (6) noted that the sedimentation velocity of rat liver oligonucleosomes underwent a "jump" between the penta- and heptanucleosome. This suggests that some new state of compaction is possible with the larger polynucleosomes, consistent, for example, with the completion of one turn of a simple superhelix or solenoid. Similar sedimentation results were obtained with chicken erythrocyte chromatin (2). In an attempt to understand this effect, we have examined the structure of tetra- to heptanucleosomes in different NaCl concentrations using the mica-replica technique. No obvious differences in morphology between these size classes were seen during salt-induced compaction (not shown), suggesting that the sedimentation

"jump" arises from a rather subtle change in conformation.

Under certain conditions, chromatin fibers in the form of strings of discrete clusters of nucleosomes (superbeads) are frequently observed (23, 27, 32, 33, 47, 48). From the compact zig-zag ribbon, the loss or weakening of one nucleosome–nucleosome contact would lead to a discontinuity in the ribbon, and a series of appropriately spaced discontinuities would produce the superbead type of structure. Fig. 1 *b–e* illustrates interruptions of this nature in the ribbon, and in Fig. 2 *b* and *d* and Fig. 7 *c* and *d*, similar breaks in the structure of isolated fibers are present. Local variations in linker DNA length are likely to result in irregularities in fiber topology, leading to the "knobby" structures which have often been reported (28). Finally, it is worth noting that fibers based on zig-zag ribbon are constructed from dinucleosome units, and are thus compatible with observations that DNase I, especially if cross-linked to a large molecule, tends to produce fragments based on the dinucleosome length (4, 5, 13).

Ubiquity of the Helical Ribbon

It is clearly premature to suggest that the helical ribbon is the primary form of architecture of the 30-nm chromatin fiber. However, the presence of long stretches of zig-zag ribbon in a variety of organisms (24, 36, 46; Fig. 1 *e–f*) suggests that this is the underlying structure of much eucaryotic chromatin. Langmore and Paulson (15) also concluded that their x-ray data were consistent with a single basic architecture. From the compact ribbon (Fig. 8), the generation of "superbeads," or coiled structures with differing degrees of compaction is a simple matter; it is not possible, however, to create a superhelical structure without first dissolving the nucleosome contacts established in the ribbon.

APPENDIX: NUCLEOSOME PACKING IN THE HELICAL RIBBON FIBER

It is possible to derive the permissible range of mass per length values for the proposed helical ribbon (Fig. 8) from helix (screw) geometry. Fig. 11 represents a regular helix after cutting parallel to the axis, and laying flat. *d* is the diameter of the original helix, *BC* is the pitch, and α the pitch angle (as defined in Fig. 4).

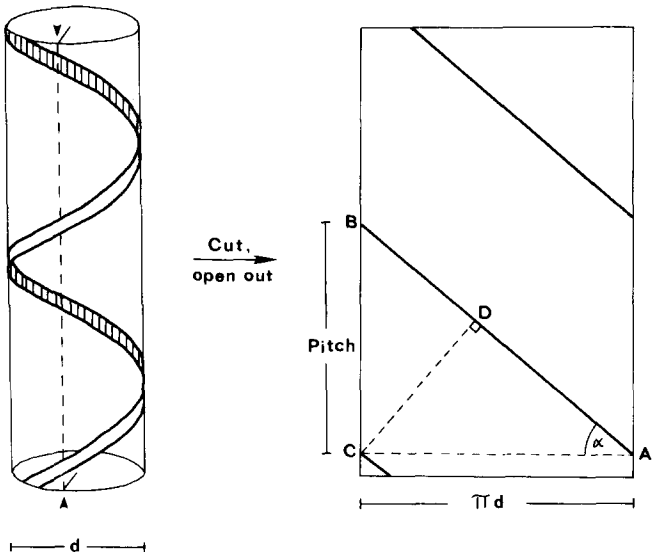

FIGURE 11 (*Left*) Representation of a regular helix. Cutting along the dotted line, followed by opening and laying flat, gives the diagram on the right.

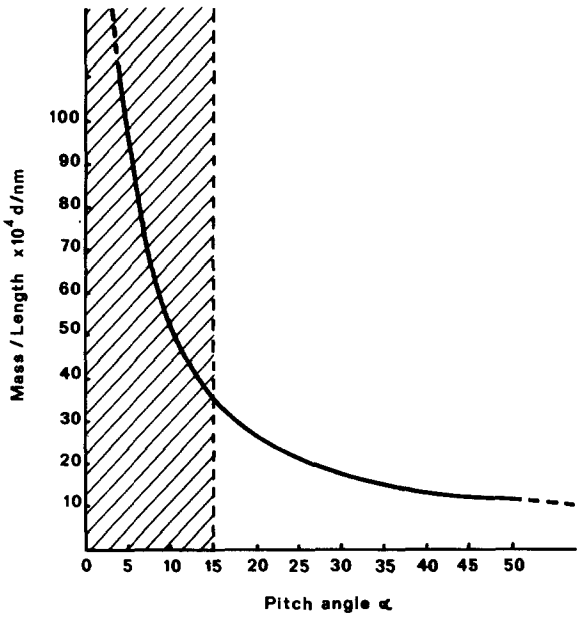

FIGURE 12 Graph of mass per length against α. Angles below 15° (shaded region) are not allowed (see text).

The mass per length is dependent on the gyre length (*AB*), the number of nucleosomes per complete gyre, and the pitch of the helix (*BC*). According to the model (Fig. 8), each gyre of the helix is constructed from the compact zig-zag ribbon, which would contain two nucleosomes/5.5 nm or 9.22×10^4 daltons/nm (Table II). Hence the mass per length of the fiber is given by

$$\text{mass per length} = \frac{AB}{BC} \cdot 9.22 \times 10^4 \text{ or } \frac{9.22 \times 10^4}{\text{Sin}\alpha} \text{ daltons/nm.}$$

A plot of mass per length against α is shown in Fig. 12.

Low values of α, leading to high mass per length values, are clearly not possible in a helix with finite gyre width. In the case of the helical ribbon, the gyre width is the width of the compact zig-zag ribbon, ~25 nm. If *CD* in Fig. 11 is 25 nm, and $d = 30$ nm, we obtain $\text{Sin}\,\alpha = (CD)/(d)$, and $\alpha = 15°$.

Under these conditions, the mass per length of the fiber ranges from 9.22×10^4 daltons/nm for the uncoiled zig-zag ribbon to 35×10^4 daltons/nm for the coiled fiber with $\alpha = 15°$ (Fig. 12). Our STEM measurements (Table I), giving mass per length values up to 27×10^4 daltons/nm, are thus consistent with the proposed helical ribbon structure.

We thank Lonny S. Jarrett for important contributions to the early stages of this work and George F. Drake for designing the freeze-drying temperature and vacuum control systems. Also, we thank James D. McGhee for many helpful suggestions in the preparation of the manuscript. We are grateful to the staff of the Brookhaven STEM facility, J. S. Wall and J. Hainfeld for advice and discussions, K. Chun for specimen preparation, F. Kito for STEM operation, E. Desmond for computer analysis, and G. Latham for the tobacco mosaic virus standard.

This study was supported by grants PCM81-04079 from the National Science Foundation and GM-25305 from the National Institutes of Health to Dr. Woodcock. Dr. Rattner is an Alberta Heritage Scholar supported by the Alberta Heritage Foundation for Medical Research and the Alberta Cancer Hospital Board. The Brookhaven STEM is supported by grant RR-00715 from the National Institutes of Health Biotechnology Resources Branch.

Received for publication 29 November 1983, and in revised form 23 March 1984.

REFERENCES

1. Allan, J., P. G. Hartman, C. Crane-Robinson, and F. X. Aviles. 1980. The structure of histone H1 and its location in chromatin. *Nature (Lond.).* 288:675–679.
2. Bates, D. L., P. J. G. Butler, E. G. Pearson, and J. O. Thomas. 1981. Stability of the higher order structure of chicken erythrocyte chromatin in solution. *Eur. J. Biochem.* 119:469–476.

3. Boulikas, T., J. M. Wiseman, and W. T. Garrard. 1980. Points of contact between histone H1 and the histone octamer. *Proc. Natl. Acad. Sci. USA.* 77:127–132.
4. Burgoyne, L. A., and J. D. Skinner. 1982. Avian erythrocyte chromatin degradation: the progressive exposure of the dinucleosome repeat by bovine-pancreatic-DNase I-armed probes and free DNase I. *Nucleic Acids Res.* 10:665–674.
5. Burgoyne, L. A., and J. D. Skinner. 1981. Chromatin superstructure: the next level of structure above the nucleosome has an alternating character. *Biochem. Biophys. Res. Commun.* 99:893–899.
6. Butler, P. J. G., and J. O. Thomas. 1980. Changes in chromatin folding in solution. *J. Mol. Biol.* 140:505–529.
7. Campbell, A. M., R. I. Cotter, and J. F. Pardon. 1978. Light scattering measurements supporting helical structures for chromatin in solution. *Nucleic Acids Res.* 5:1571–1580.
8. Carpenter, B. G., J. P. Baldwin, E. M. Bradbury, and K. Ibel. 1976. Organization of subunits in chromatin. *Nucleic Acids Res.* 3:1739–1746.
9. Christiansen, G., and J. Griffith. 1977. Salt and divalent cations affect the flexible nature of the natural beaded chromatin structure. *Nucleic Acids Res.* 4:1837–1851.
10. Finch, J. T., and A. Klug. 1976. Solenoidal model for superstructure in chromatin. *Proc. Natl. Acad. Sci. USA.* 73:1897–1901.
11. Frado, L-L. Y., C. L. F. Woodcock, C. V. Mura, and B. D. Stollar. 1983. Mapping of histone H5 sites on nucleosomes using immunoelectron microscopy. *J. Biol. Chem.* 258:11984–11990.
12. Igo-Kemenes, T., W. Horz, and H. G. Zachau. 1982. Chromatin. *Annu. Rev. Biochem.* 51:89–121.
13. Khachatrma, A. T., V. A. Pospelov, S. B. Svetlikova, and V. I. Vorob'ev. 1981. Nucleodisome—a new repeat unit of chromatin revealed in nuclei of pigeon erythrocytes by DNase I digestion. *FEBS (Fed. Eur. Biochem. Soc.) Lett.* 128:90–92.
14. Kornberg, R. D. 1977. Structure of chromatin. *Annu. Rev. Biochem.* 46:931–934.
15. Langmore, J. P., and J. R. Paulson. 1983. Low angle x-ray diffraction studies of chromatin structure in vivo and in isolated nuclei and metaphase chromosomes. *J. Cell Biol.* 96:1120–1131.
16. Lee, K. S., M. Mandelkern, and D. M. Crothers. 1981. Solution structure studies of chromatin fibers. *Biochemistry.* 20:1438–1445.
17. McGhee, J. D., and G. Felsenfeld. 1980. Nucleosome structure. *Annu. Rev. Biochem.* 49:1115–1156.
18. McGhee, J. D., J. M. Nickol, G. Felsenfeld, and D. C. Rao. 1983. The higher order structure of chromatin: the orientation of nucleosomes within the 30 nm chromatin solenoid is independent of species and spacer length. *Cell.* 33:831–841.
19. McGhee, J. D., D. C. Rau, E. Charney, and G. Felsenfeld. 1980. Orientation of the nucleosome within the higher order structure of chromatin. *Cell.* 22:87–96.
20. Murcia, G., and T. Koller. 1981. The electron microscopic appearance of soluble rat liver chromatin mounted on different supports. *Biol. Cell.* 40:165–174.
21. Olins, A. L., and D. E. Olins. 1979. Stereoelectron microscopy of the 25 nm chromatin fibers in isolated nuclei. *J. Cell Biol.* 81:260–265.
22. Pearson, E. C., P. J. G. Butler, and J. O. Thomas. 1983. Higher order structure of nucleosome oligomers from short repeat chromatin. *EMBO (Eur. Mol. Biol. Organ.) J.* 2:1367–1372.
23. Pruitt, S. C., and R. M. Grainger. 1980. A repeating unit of higher order chromatin structure in chick red blood cell nuclei. *Chromosoma (Berl.).* 78:257–274.
24. Rattner, J. B., and B. A. Hamkalo. 1978. Higher order structures in metaphase chromosomes I The 250A fiber. *Chromosoma (Berl.).* 69:373–379.
25. Rattner, J. B., and B. A. Hamkalo. 1979. Nucleosome packing in interphase chromatin. *J. Cell Biol.* 81:453–457.
26. Rattner, J. B., C. Saunders, and J. R. Davie. 1982. Ultrastructure organization of yeast chromatin. *J. Cell Biol.* 93:217–222.
27. Renz, M., P. Nehls, and J. Hozier. 1977. Involvement of histone H1 in the organization of the chromosome fiber. *Proc. Natl. Acad. Sci. USA.* 74:1879–1884.
28. Ris, H., and J. Korenberg. 1979. Chromosome structure and levels of organization. *In* Cell Biology, Vol. 2. D. M. Prescott and L. Goldstein, editors, Academic Press, Inc., New York. 268–361.
29. Ruiz-Carillo, A., P. Puigdomenech, G. Eder, and R. Lurz. 1980. Stability and reversibility of higher ordered structure of interphase chromatin: continuity of DNA is not required for maintenance of folded structure. *Biochemistry.* 19:2544–2554.
30. Simpson, R. T. 1978. Structure of the chromatosome, a particle containing 160 bp of DNA and all the histones. *Biochemistry.* 17:5524–5531.
31. Stein, A. 1980. DNA wrapping nucleosomes: the linking number reexamined. *Nucleic Acids Res.* 8:4803–4820.
32. Stratling, W. H., and R. Klingholz. 1981. Supranucleosomal structure of chromatin: digestion by calcium/magnesium endonuclease proceeds via a discrete size class of particles with elevated stability. *Biochemistry.* 20:1386–1392.
33. Stratling, W. H., U. Muller, and H. Zentgraf. 1978. The higher order repeat structure of chromatin is built up of globular particles containing eight nucleosomes. *Exp. Cell Res.* 117:301–311.
34. Subirana, J. A., S. Munoz-Guerra, M. Radermacher, and J. Frank. 1983. Three dimensional reconstruction of chromatin fibers. *J. Biomol. Struct. Dynam.* In press.
35. Thoma, F., and T. Koller. 1977. Influence of H1 on chromatin structure. *Cell.* 12:101–107.
36. Thoma, F., T. Koller, and A. Klug. 1979. Involvement of histone H1 in the organization of the nucleosome, and the salt-dependent substructures of chromatin. *J. Cell Biol.* 83:408–427.
37. Thomas, J. O., and A. J. A. Khazaba. 1981. Cross-linking of histone H1 in chromatin. *Eur. J. Biochem.* 112:501–511.
38. Thomas, J. O., and R. J. Thompson. 1977. Variation in chromatin structure in two cell types from the same tissue: a short DNA repeat length in cerebral cortex neurons. *Cell.* 10:633–640.
39. Tyler, J. M., and D. Branton. 1980. Rotary shadowing of extended molecules dried from glycerol. *J. Ultrastruct. Res.* 71:95–103.
40. Wang, J. C. 1982. The path of DNA in the nucleosome. *Cell.* 29:724–726.
41. Wall, J., and J. Hainfield. 1978. A new STEM capable of observing single heavy atoms in frozen biological specimens. *In* Proceedings 9th International Congress of Electron Microscopy. J. M. Sturgess, editor. Microscopical Society of Canada. 16–17.
42. Woodcock, C. L. F., L-L. Y. Frado, G. R. Green, and L. Einck. 1981. Adhesion of particulate specimens to support films for electron microscopy. *J. Microsc. (Oxf.).* 121:211–220.
43. Woodcock, C. L. F., L-L. Y. Frado, and J. S. Wall. 1980. Composition of native and reconstituted chromatin particles: direct mass determination using scanning transmission electron microscopy. *Proc. Natl. Acad. Sci. USA.* 77:4818–4822.
44. Woodcock, C. L. F., and L. S. Jarrett. 1981. Packing of nucleosomes in the 25 nm chromatin fiber. *J. Cell Biol.* 91:57*a*. (Abstr.)
45. Worcel, A., and C. Benyajati. 1977. Higher order coiling of DNA in chromatin. *Cell.* 12:83–100.
46. Worcel, A., S. Strogartz, and D. Riley. 1981. Structure of chromatin and the linking number of DNA. *Proc. Natl. Acad. Sci. USA.* 78:1461–1465.
47. Zentgraf, H., V. Muller, and W. W. Franke. 1980. Supranucleosomal organization of sea urchin sperm chromatin in regularly arranged 40 to 50 nm large granular subunits. *Eur. J. Cell Biol.* 20:254–264.
48. Zentgraf, H., U. Muller, and W. W. Franke. 1980. Reversible *in vitro* packing of nucleosomal filaments into globular supranucleosomal units in chromatin of whole chick erythrocyte nuclei. *Eur. J. Cell Biol.* 23:171–188.